Department of Precision and Microsystems Engineering

Synthesis of a Force Generator using Two-Fold Tape Loops

M.G. de Jong

Report no : 2018.008
Coach : Ir. W.W.P.J. van de Sande
Professor : Prof. dr. ir. J.L. Herder
Specialisation : Mechatronic System Design
Type of report : Master Thesis
Date : 17 May 2018

Synthesis of a Force Generator using Two-Fold Tape Loops

by

M.G. de Jong

in partial fulfillment of the requirements for the degree of

Master of Science

in Mechanical Engineering

at the Delft University of Technology,

to be defended publicly on Thursday May 17, 2018 at 2:00 PM.

Student number:	4169646	
Thesis committee:	Prof. dr. ir. J.L. Herder,	TU Delft, Chair
	Ir. W.W.P.J. van de Sande,	TU Delft, Supervisor
	Dr. ir. T. Horeman,	TU Delft
	Ir. F. Baas,	InteSpring

TU Delft Delft University of Technology

Preface

This thesis is the final result of the master Precision and Microsystem Engineering at the faculty of Mechanical, Maritime and Material Engineering at the Delft University of Technology. I once started my study career at Business Administration at the the Erasmus University in Rotterdam and I have always insisted that after I finished my bachelor in Mechanical Engineering, I would go back to the economical studies. I had never expected that I would end this study career by graduating in one of the most technical disciplines here in Delft. I would like to express my deepest gratitude to the people who have been of a great support during my whole study and especially during this last year.

I would like to thank my daily supervisor Werner for being a great brainstorming partner, for giving me fresh energy after each meeting and for reviewing my work over and over again. I would like to thank Just for his feedback during the meetings and for helping me keeping the right focus. I would like to thank the people of InteSpring, especially Frank and my fellow interns, who provided me my portion of weekly feedback during the weekly student update. I would like to thank Gerard and René of the workshop for thinking along in the production process. I would like to thank Patrick and Harry who helped me with setting up the experiment. I would like to thank Rick en Liora who have always invited me for diner when I was too busy, writing this thesis, for cooking. I would like to thank Henri for being my graduation soul mate and for reviewing my work. I would like to thank my family for all the support they have given. Finally I would like to thank my girlfriend who has always provided me the right conditions so I could perform my thesis writing and supported me in every way possible.

M.G. de Jong
Delft, May 2018

Contents

1

Introduction

Normal springs, as shown in figure 1.1a, are often considered as elements that behave according to Hooke's law. This law states that the spring characteristic is linear, i.e. $F = kx$. This characteristic is not always adequate in complex applications. For instance in static balancing applications, constant force or negative stiff spring elements are desired [1]. There are also applications where stiffening/softening or multistable behavior is desired.

There are specific solutions for each characteristic, such as coiled constant force springs [2] or buckled leaf springs [3]. These mechanisms are solutions for one application. There are also mechanisms that can have multiple characteristics, such as cam follower mechanisms [4]. These mechanisms can be called force generators with a custom force displacement behavior, because their force displacement curve can be adjusted. The downside of these mechanisms is that they usually consist of many parts and are limited scalable. A compliant variant of such a mechanism could possibly lower the number of parts and improve scalability.

Compliant shell mechanisms are mechanisms that can possibly have any displacement and any force characteristic as desired. The difficulty of synthesizing compliant shell mechanisms is to match both the required displacement and the required force behavior, while they are both not restricted.

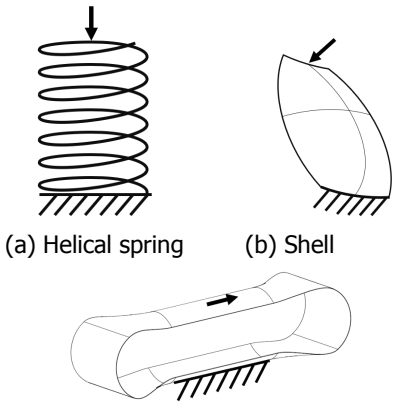

(a) Helical spring (b) Shell

(c) Tape spring

Figure 1.1: Different spring elements

A tape loop, as shown in figure 1.1c, is one type of compliant shell mechanism where the input motion is restricted to a linear motion, which results in a linear guide [5]. By restricting the displacement, the synthesis method can be focused on the force behavior, which results in a less complex synthesis process. A tape loop consists of a double folded tape spring which is clamped at one side and actuated at the other side. When a tape spring with a constant width is used, the strain energy within the tape spring does not change when a motion is applied. However, when varying the width of the tape spring, the strain energy changes during motion. In this way a very compact and monolithic force generator can be designed.

In this thesis fifteen force displacement curves are identified which all describe a unique force displacement behavior. These fifteen curves are used to quantify the level of customizability of force generators. Before force generators are created from a tape loop by varying the cross-section, the influence of the cross-section on the tape loop's behavior is investigated. The two main subjects that are investigated are the energy state of a tape spring and the tape spring radius. The knowledge of the energy state is necessary for the synthesis method. The dependency of the tape spring radius on the cross-section is investigated, to assure a pure horizontal motion, which is required for a tape loop

to act as a linear guide. With this knowledge, a synthesis method for a force generator using tape loops is developed. This synthesis method is used to synthesize fifteen tape loops with each having one of the fifteen unique force displacement behaviors.

Thesis Outline

The main work of this thesis consists of three chapters. Two of these chapters are written as stand-alone papers and therefore there is some overlap between these papers.

Chapter two explains what force generators with custom force displacement behavior are and gives examples of existing force generators. In this chapter, the fifteen force displacement curves are presented and used to quantify the customizability of the found force generators.

The third chapter, which is the first paper, investigates the influence of the tape spring's cross-section on several characteristics of a folded tape spring such as the fold angle, the fold radius and the energy distribution.

The fourth chapter, which is the second paper, uses the knowledge of the third chapter to synthesize a force generator with custom force displacement behavior using a folded tape spring by adjusting its cross-section. The fifteen force displacement curves of the introducing chapter are used to check in what level the tape loop can be customized. One of the fifteen geometries is optimized for the rquired behavior, produced and tested in an experiment.

The thesis ends with a discussion and conclusion. Several appendices are attached which give more explanation on the production, simulation and experiments.

2

Force Generators with Custom Force Displacement Behavior

FORCE GENERATORS WITH CUSTOM FORCE DISPLACEMENT BEHAVIOR

Marinus G. de Jong
Dept. of Precision and Microsystems Engineering
Delft University of Technology
Delft, 2628 CD, The Netherlands
Email: M.G.deJong@tudelft.nl

Werner W.P.J. van de Sande
Just L. Herder
Dept. of Precision and Microsystems Engineering
Delft University of Technology
Delft, 2628 CD, The Netherlands
W.W.P.J.vandeSande@tudelft.nl, J.L.Herder@tudelft.nl

INTRODUCTION

Force generators are mechanisms that generate a force at a certain point which is referred to as the input of the mechanism. When all of the work done at the input is absorbed as strain energy within the mechanism, the force generator is called a spring. Most of the basic springs are linear and behave according to Hooke's law. However, there are situations where linear springs do not have the right load-displacement behavior. For instance when balancing a weight vertically in one direction, a constant force spring is needed [1], [2]. When balancing the human body with a wearable device, the required load displacement is even more complex [3], [4], [5]. There are solutions using active controlling to obtain the required load displacement [6], [7], [8]. However, this usually results in a bulky and heavy system. Therefore passive force generators with a custom load-displacement path are more suitable for these kind of applications.

This chapter gives an overview of the custom nonlinear spring elements that are currently available. In the next section the scope of this chapter and the way the literature search is performed will be explained. A categorization is derived and the force displacement curves are introduced. In the third section, the found mechanisms are presented and are grouped into categories based on their working principle. The mechanisms are analyzed using the defined force displacement curves and criteria. The chapter ends with a discussion and conclusion.

METHOD

Scope

Within this review, only force generators that store their energy in the form of strain energy are included. Furthermore the force generators may not contain any active controlling elements. Only continuous mechanisms are in the scope of this review. The customization of the spring characteristics should be more than only scaling or (phase)shifting the load-displacement curve.

TABLE 1. KEYWORDS USED IN LITERATURE SEARCH.

AND	AND	AND	AND
adjustable	”force displacement”	energy	negative
variable	”force generat*”	stiffness	zero
tun*able	”force mechanism”		constant
tailored	spring*		nonlinear
	”load displacement”		{non-linear}

Literature Search

A literature search was performed using the Scopus database and the TUDelft Library catalogue. The search terms that were used to search in the title, abstract and keywords are listed in Tab. 1. Besides these including terms, the following terms were used to exclude literature when these terms are in the title: *electr*, active, motor, controller, magnet*, damp*, hydr*, composite, muscle* and aerodynamic*. From the relevant articles, the cited references were reviewed to find other relevant articles.

Categorization

The categorization is based on the way how the potential energy at a certain displacement can be influenced. The most basic function of potential energy stored within a spring element

as a function of displacement x is given by

$$U(x) = \frac{1}{2}kx^2, \tag{1}$$

which is completely determined when stiffness k is constant. However, the goal within this paper is to find mechanisms where the potential energy can be freely determined independently of the displacement. This can be done in two ways: add an extra displacement dependent term or make the stiffness dependent on the displacement:

$$U(x) = \frac{1}{2}k\big(x+C(x)\big)^2 \tag{2}$$

$$U(x) = \frac{1}{2}k(x)x^2. \tag{3}$$

The extra $C(x)$ term can be interpreted as a transmission between the displacement and the spring element. The basic formula of the stiffness term k, using bending stiffness is

$$k = EI, \tag{4}$$

where E is the Young's modulus which is a material property and I is the second moment of area which is a geometry property. If one of these terms is displacement dependent, the stiffness will not be constant anymore, which will influence the stored potential energy at a certain location. Figure 1 summarizes the categorization.

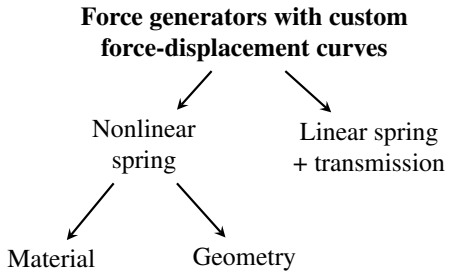

FIGURE 1. CATEGORIZATION OF FORCE GENERATORS WITH CUSTOM FORCE-DISPLACEMENT CURVES.

Force-Displacement Curves

Radaelli [9] defined a set of possible nonlinear force-displacement curves. These force-displacement curves are based on the force, stiffness and derivative of stiffness which can either be negative, zero or positive, resulting in twenty seven different curves. Twelve of these twenty seven force-displacement curves are not unique, because they can be obtained by mirroring another curve. This means that the definition of the direction of the force and displacement of a mechanism are mirrored, which physically does not change the mechanism itself. This symmetry results in fifteen unique force-displacement curves.These fifteen curves will be used to quantify the level of customization of the mechanisms.

Criteria

Besides the achievable force-displacement curves, the mechanisms will be given a score based on the following criteria.

Adjustability after fabrication The way the load-displacement curve can be adjusted after the mechanism is produced. This adjustability of the load-displacement curved mostly consists of scaling or (phase) shifting the curve.

Complexity of mechanism The complexity of the mechanism itself is defined by the number of parts and the manufacturability. The number of part is given a score of 'high', 'medium', 'low' or 'one'. The manufacturability is given a score between 1 and 5.

Complexity of synthesis method The complexity of the synthesis method is given a score between 1 and 3. When there is an analytical solution of finding the dimensions of mechanism to obtain the required characteristics, the synthesis method is relatively easy, so the score of 1 is given. When an iterative method is required to find the right design, but the relation is clearly defined, the score of 2 is given. When an optimization algorithm is required to find the right design, the synthesis method is quit complex, so a score of 3 is given.

RESULTS

Mechanisms

Figure 2 shows the schematic representations of the found examples of force generators with custom force-displacement behavior. The axis of the mechanisms are given for each mechanism, where the y-direction is mostly in the direction of the spring element and the x-dimension is the second dominant dimension.

Based on the categorization in Fig. 1, there are three ways to create a mechanism with a custom energy-displacement curve: Nonlinear spring due to the material properties, nonlinear spring due to the geometry and linear spring with a nonlinear transmission. The mechanisms that will be shortly described by means of these working principles.

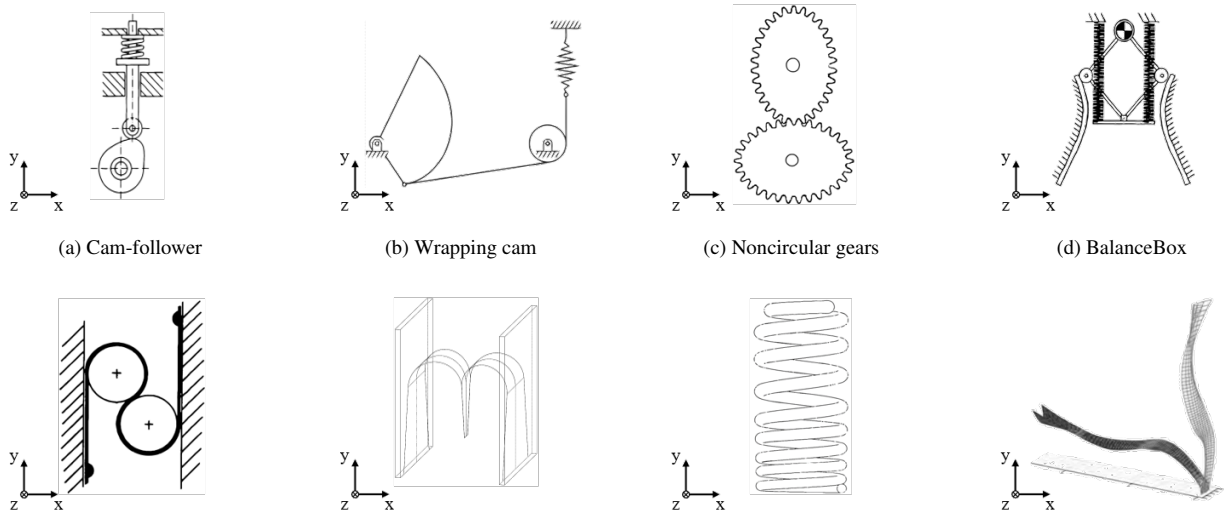

(a) Cam-follower (b) Wrapping cam (c) Noncircular gears (d) BalanceBox

(e) Rolamite (f) Two bent leaf springs (g) Nonlinear helical spring (h) Freeform compliant

FIGURE 2. SCHEMATIC REPRESENTATIONS OF FORCE GENERATORS WITH CUSTOM ENERGY-DISPLACEMENT CURVES. UPPER ROW IS NONLINEAR DUE TO A TRANSMISSION BETWEEN INPUT MOTION AND ENERGY STORAGE ELEMENT. LOWER ROW IS NONLINEAR DUE TO THE GEOMETRY OF THE ENERGY STORAGE ELEMENT ITSELF.

Cam-Follower [10], [11] The input motion is a rotation of a non-circular cam which pushes a linear spring. The shape of the cam determines the relation between the input motion and the spring length.

Wrapping Cam [12] The input motion is a rotation of a non-circular cam which pulls a linear spring by a string. The shape of the cam determines the relation between the input motion and the spring length.

Non-circular gears [13] The rotational input motion is passed on through two non-circular gears to the rotational spring. The profile of the two gears determines the ratio between the input motion and elongation of the rotational spring.

BalanceBox [14], [15] The translational input motion is converted through a parallelogram mechanism that rolls on a path. The shape of the path determines the relation between the input motion and the spring length.

Rolamite [16], [17] A steel band is bent around two rollers within a casing. The profile of the band width or the initial band curvature profile determines the strain energy a curtain displacement.

Two bent leaf springs [9] Two leaf springs are bent between walls. The profile of the leaf springs determines the amount of material that is bent at a curtain displacement and thereby the strain energy. There was no article found about this mechanism, but it is mentioned in [9].

Nonlinear helical spring [18] A 'normal' helical spring but with a nonconstant pitch, wire diameter or coil diameter.

Freeform compliant mechanisms [9], [19] There are two types of compliant mechanisms: Lumped compliant mechanisms and shells. Lumped compliant mechanisms are usually planar and are the compliant equivalents of bar linkages. Shells consist of curved planes and can act in more than two dimensions.

Criteria

The results of the comparison using the criteria are given in Tab. 2. The mechanisms where the energy storage element and the non-linearity are separated are adjustable after fabrication, because the pretension of the spring element is adjustable. This is not possible when the input motion is directly coupled to the energy storage element, as is the case at the mechanisms in the category nonlinear due to the geometry of the energy storage element.

When the non linearity is due to the geometry of the energy storage element, the mechanism can be monolithic, which is the case for the nonlinear helical spring and freeform compliant mechanisms. The BalanceBox is the most complex system in terms of number of parts.

The manufacturability is the most complex for the freeform compliant mechanisms, because such a mechanism can result in an unorthodox geometry which requires complex production methods.

For the rolamite and the two bent leaf springs, the geometry can be analytically determined, which makes the synthesis method relatively easy. Because both the force and the displacement path of a freeform compliant mechanism are not defined, the synthesis method is very complex. The other mechanisms need to be synthesized in an iterative way.

Force Displacement Curves

Table 3 shows the comparison of the different mechanisms using the fifteen force-displacement curves.The wrapping cam and noncircular gear cannot change the direction of the torque and they can also not have a zero torque. The mechanism with two bent leaf springs can only pull, so the curves with both negative and positive forces cannot be achieved. The nonlinear helical spring can only have a linear or progressive positive stiffness.

DISCUSSION

For most of the mechanisms, it is not documented which force displacement curves they can achieve. Therefore the process of identifying the possible force displacement curves is somewhat subjective. The method showed however that the fifteen unique force displacement curves can be used to compare different force generators with a custom force displacement path.

CONCLUSION

An overview is presented of force generators with a custom force displacement path that are available. The mechanisms are categorized, based on how the input motion can be decoupled from the strain energy: due to the material properties, due to its geometry and due to a nonlinear transmission. Four mechanisms that can be customized due to its geometry and four mechanisms that can be customized due tot a nonlinear transmission have been found. There was no mechanism found that could be customized by changing the material properties.

Fifteen unique force displacement curves were used to quantify the force displacement behavior of the mechanisms. Some of the mechanisms can theoretically achieve all curves (Cam-Follower, BalanceBox, Rolamite and Freeform Compliant), while others are limited.

The mechanisms were also compared using criteria. The mechanisms that were based on a nonlinear transmission could all be adjusted after fabrication, while all mechanisms that were based on the geometry could not be adjusted.

REFERENCES

[1] Herder, J., 2001. “Energy-free systems: theory, conception, and design of statically balanced spring mechanisms”. Phd thesis, Delft University of Technology.

[2] French, M. J., and Widden, M. B., 2000. “The spring-and-lever balancing mechanism, George Carwardine and the Anglepoise lamp”. *Institution of Mechanical Engineers, Part C: Journal of Mechanical Engineering Science,* ***214***, pp. 501–508.

[3] Dicharry, J., 2010. “Kinematics and Kinetics of Gait: From Lab to Clinic”. *Clinics in Sports Medicine,* ***29***(3), pp. 347–364.

[4] De Vlugt, E., de Groot, J. H., Wisman, W. H. J., and Meskers, C. G. M., 2012. “Clonus is explained from increased reflex gain and enlarged tissue viscoelasticity”. *Journal of Biomechanics,* ***45***, pp. 148–155.

[5] Yamamoto, S., Ebina, M., Miyazaki, S., Kawai, H., and Kubota, T., 1997. “Development of a New Ankle-Foot Orthosis with Dorsiflexion Assist, Part 1: Desirable Characteristics of Ankle-Foot Orthoses for Hemiplegic Patients”. *Journal of Prosthetics and Orthotics,* ***9***(4), pp. 174–179.

[6] Zoss, A. B., Kazerooni, H., and Chu, A., 2006. “Biomechanical Design of the Berkeley Lower Extremity Exoskeletong (BLEEX)”. *IEEE/ASME Transactions on Mechatronics,* ***11***(2), pp. 128–138.

[7] Huang, J., Tu, X., and He, J., 2016. “Design and Evaluation of the RUPERT Wearable Upper Extremity Exoskeleton Robot for Clinical and In-Home Therapies”. *IEEE Transactions on Systems, Man, and Cybernetics: Systems,* ***46***(7), pp. 926–935.

[8] Jo, I., and Bae, J., 2017. “Design and control of a wearable and force-controllable hand exoskeleton system”. *Mechatronics,* ***41***, pp. 90–101.

[9] Radaelli, G., 2017. “Synthesis of Mechanisms with Prescribed Elastic Load-Displacement Characteristics”. Phd thesis, Delft University of Technology.

[10] Mills, J., Notash, L., and Fenton, R., 1993. “Optimal Design and Sensitivity Analysis of Flexible Cam Mechanisms”. *Mech. Mach. Theory,* ***28***(4), pp. 563–581.

[11] Norton, R. L., 2009. *Cam Design and Manufacturing Handbook*, 2nd editio ed. Industrial Press, Inc., New York.

[12] Kilic, M., Yazicioglu, Y., and Funda Kurtulus, D., 2012. “Synthesis of a torsional spring mechanism with mechanically adjustable stiffness using wrapping cams”. *Mechanism and Machine Theory journal,* ***57***, pp. 27–39.

[13] Litvin, F. L., Fuentes-Aznar, A., Gonzalez-Perez, I., and

TABLE 2. MECHANISM COMPARISON USING CRITERIA.

	Cam-follower	Wrapping cam	Non-circular gears	Balance-Box	Rolamite	Two bent leaf springs	Nonlinear helical spring	Freeform compli-ant
Adjustability after fabrica-tion	Yes	Yes	Yes	Yes	No	No	No	No
Complexity of mechanism by...								
number of parts	Medium	Low	Low	High	Medium	Low	One	One
manufacturabilty	2	2	2	3	3	3	4	5
Complexity of synthesis method	2	2	2	2	1	1	2	3

Hayasaka, K., 2009. *Noncircular Gears: Design and Generation*. Cambridge University Press, Cambridge.

[14] Wisse, M. B., Barents, R., van Dorsser, W. D., and Herder, J. L., 2010. Apparatus for Exercising a Force on a Load.

[15] Thomas Regout International, 2018. BalanceBox.

[16] Cadman, R. V., 1970. Rolamite - Geometry and Force Analysis. Tech. rep., Sandia Laboratories, Albuquerque, N. Mex.

[17] English, C., and Russell, D., 1999. "Implementation of variable joint stiffness through antagonistic actuation using rolamite springs". *Mechanism and Machine Theory,* ***34***, pp. 27–40.

[18] Ji, J., Li, Y., and Zhao, J., 2011. "Reverse Analysis for Determining the Stiffness Characteristics of Suspension Spring with Variable Pitch and Wire Diameter". *Advanced Materials Research,* ***421***, pp. 783–787.

[19] Jutte, C. V., 2008. "Generalized Synthesis Methodology of Nonlinear Springs for Prescribed Load-Displacement Functions". Phd thesis, University of Michigan.

TABLE 3. MECHANISM COMPARISON USING ENERGY CURVES. GRAY CELLS MARK THEORETICAL ACHIEVABLE CURVES. NOTE THAT THE ENERGY LEVELS CAN BE FREELY CHOSEN, THUS THE CROSSINGS WITH THE X-AXIS HAVE NO PARTICULAR MEANING.

		Linear spring + transmission				**Nonlinear spring due to geometry**			
		Cam-follower	Wrapping cam	Noncircular gears	Balance-Box	Rolamite	Two bent leaf springs	Nonlinear helical spring	Freeform compli-ant
Positive stiffness									
Positive & negative or zero stiffness									
Negative stiffness	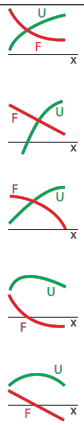								

3

Paper: Influence of the Subtended Angle on the Behavior of Folded Tape Springs

This paper is submitted and accepted to the ASME 2018 International Design Engineering Technical Conferences & Computers and Information in Engineering Conference.

Proceedings of the ASME 2018 International Design Engineering Technical Conferences & Computers and Information in Engineering Conference
IDETC/CIE 2018
August 26-29, 2018, Quebec City, Canada

DETC2018-86159

INFLUENCE OF THE SUBTENDED ANGLE ON THE BEHAVIOR OF FOLDED TAPE SPRINGS

Marinus G. de Jong
Dept. of Precision and Microsystems Engineering
Delft University of Technology
Delft, 2628 CD, The Netherlands
Email: M.G.deJong@tudelft.nl

Werner W.P.J. van de Sande*
Just L. Herder
Dept. of Precision and Microsystems Engineering
Delft University of Technology
Delft, 2628 CD, The Netherlands
W.W.P.J.vandeSande@tudelft.nl, J.L.Herder@tudelft.nl

ABSTRACT

Tape springs are thin-walled structures with zero longitudinal and constant transverse curvature. Folding them twice and connecting both ends creates a tape loop which acts as a linear guide. When using a tape spring with a non-constant cross-section, a force generator can be created. At this time there is insufficient understanding of the influence of the tape spring's cross-section on its behavior. This study investigates the influence of the subtended angle on the tape spring's behavior, especially the energy distribution and the fold radius.

A tape spring is once folded in a finite element model. By performing a curvature analysis of this folded geometry, the different regions within a tape spring are identified. This information is used to identify the amount of strain energy of each region. Finally, the fold radius and fold angle are determined by analyzing the geometry of the bent region.

The analysis showed that the energy within the transition regions cannot be neglected. The energy within these regions as ratio of the total energy and the length of the transition regions both increase with the subtended angle. It is also shown that the fold radius is not constant when the subtended angle is small.

Therefore, when designing a force generator using tape loops, the energy within the transition regions should be taken into account. The subtended angle should not be small to ensure a constant radius.

*Address all correspondence to this author.

INTRODUCTION

Compliant mechanisms are mechanisms that move due to elastic deformation of slender segments. These mechanisms have advantages compared to traditional mechanisms such as reduced wear, reduced or eliminated backlash, no need for lubrication and possibilities for monolithic designs [1].

Most compliant mechanisms consist of beam flexures that move in a plane, such as compliant grippers [2] and MEMS devices [3]. A relatively new area in the field of compliant mechanisms is that of shell mechanisms. These mechanisms have curved flexures and have complex shapes and kinetics [4].

As shells are defined as curved thin-walled structures, one of the most basic shell elements is a tape spring: a thin-walled open cylindrical structure with zero longitudinal and constant transverse curvature. A carpenters tape is an example of such geometry. Despite its simple geometry, a tape spring has some remarkable properties, such as being stiff before buckling while being compliant after buckling, having a constant fold radius [5] and constant moment after buckling [6]. Because of these properties, tape springs are used as hinges [7] or as deployable stiff structures in space [8].

A special configuration of a folded tape spring is a tape loop, which is a tape spring with multiple folds and its ends connected to each other. Vehar [9] examined different setups with a different number of folds. The simplest configuration of a tape loop is with two folds, which acts as a zero force and zero stiffness linear guide as explored by Houwers [10].

A two folded tape loop is the monolithical equivalent of a rolamite, which has the same working principle [11]. A rolamite can act as force generator by changing the geometry of the band [12, 13]. In further analogy to the rolamite, a tape loop can be turned into a force generator by changing the cross section of the tape spring. Radaelli [14] suggested a constant force mechanism using a two-fold tape loop with a tapered tape spring. However, to make a more generic force generator out of a tape loop, more insight into the influence of the tape spring's cross section on its energy state is desired.

Quite some theoretical research has been performed on tape spring buckling [15], deployment dynamics [6] and the fold curvature [16]. Seffen derived an analytical formula of the strain energy within the bent region of a tape spring [17]. The bent region however is not the only region where strain energy is stored. There is also a transition region between the undeformed region and the bent region, which contains an amount of strain energy.

The total energy state of the tape loop should be known when using tape springs as a force generator. Therefore the energy within the transition region should be investigated to determine whether it can be neglected or not. Another important factor to determine is whether the fold radius remains constant while varying the cross-section, since otherwise the tape loop will not act as a straight-line guide.

This paper will investigate the influence of the tape spring's cross-section on the total energy state and the geometry of a single folded tape spring. The cross-section is adjusted by varying the subtended angle, which is the angle in transverse direction of the tape spring. In order to do investigate the influence of the subtended angle, several tape springs are simulated in a finite element method (FEM) model, where all variables are kept constant except the subtended angle. The tape spring will be folded 180 degrees as to act as the half of a tape loop. By performing a curvature analysis, the different regions of a tape spring are identified. With this information, the energy within the different regions can be identified. Finally, the effect of the subtended angle on the geometry in the bent region will be analyzed.

This paper starts with the basic theory of a folded tape spring. Then the methods used in analysis are explained. Subsequently, the results of the FEM analysis are showed. In the discussion, the influence of the results to the synthesis method of a force generator using tape loops is discussed. Finally the paper concludes with some remarks.

METHOD

Tape Spring Basics

Parameters of a Folded Tape Spring. A tape spring fold is created by applying a moment to both ends of a tape spring. A tape spring can be folded into two directions: equal sense or opposite sense. The fold is called equal sense when the open sides of the tape spring are facing towards each other and vice versa [17]. Figure 1 shows an equal sense folded tape spring together with its original geometry. The undeformed geometry has a constant transverse radius R and zero longitudinal radius with a so-called subtended angle α, thickness t and length L. From now on the transverse radius will be called the tape spring radius. The folded geometry has a fold radius R^* with a fold angle θ.

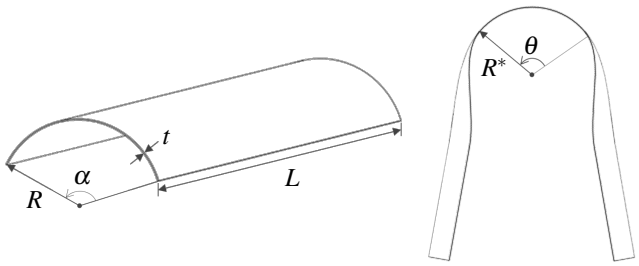

(a) Undeformed tape spring (b) Folded tape spring

FIGURE 1. PARAMETERS OF AN EQUAL SENSE FOLDED TAPE SPRING.

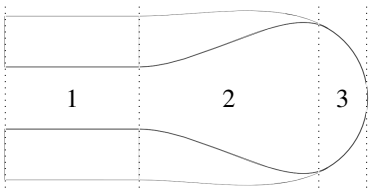

FIGURE 2. DIFFERENT REGIONS WITHIN A FOLDED TAPE SPRING: 1) UNDEFORMED REGION, 2) TRANSITION REGION, 3) BENT REGION.

Tape Spring Regions. Three different regions can be identified within a folded tape spring. Figure 2 shows a folded tape spring with the different regions numbered.

The first region is the undeformed region. This is where the tape spring has its original shape. The second region is called the transition region. In this region the tape spring goes from the original to fully deformed shape. The third region is called the bent region. In this region the tape spring is fully deformed in both transverse and longitudinal direction.

Equation of Energy. The potential strain energy expression for a fold in a tape spring without twist, using the definitions as shown in Fig. 1 and 3, is given by

$$U = \frac{\alpha D}{2} \int_{-\theta/2}^{\theta/2} \left[\frac{R}{r(\beta)} + \frac{r(\beta)}{R} \pm 2\nu \right] d\beta \qquad (1)$$

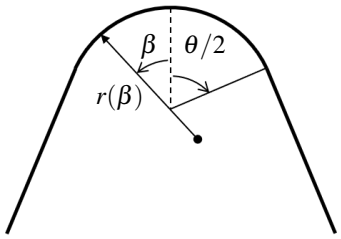

FIGURE 3. DEFINITION OF PARAMETERS ASSOCIATED WITH DEFORMATION OF A TAPE SPRING [17].

with $D = Et^3/12(1-\nu^2)$, where E is the Young's modulus and ν the Poisson's ratio [17, 18]. The plus-minus sign is for respectively opposite and equal sense bending. This equation does not take the transition regions into account, so the assumption is made that the energy within in the transition regions can be neglected.

With the use of several other assumptions, Eqn. (1) can be simplified. It has been suggested that the fold radius is constant $(r(\beta) = R^*)$ and that the fold radius R^* is equal to R [5]. Furthermore, because in this paper a single fold of a two-fold tape loop is considered, the fold angle θ can be set to π. With these assumptions, Eqn. (1) can be reduced to

$$U = \frac{\alpha \pi E t^3}{12(1 \pm \nu)} \tag{2}$$

where the plus-minus sign now represents respectively equal and opposite sense bending.

Analysis Methodology

Hypotheses. In order for Eqn. (2) to describe the energy state of the tape spring, several hypotheses need to hold:

1. The energy within the transition regions can be neglected
2. The fold radius is independent of the subtended angle and equal to the tape spring radius
3. The fold angle is independent of the subtended angle and has a constant value of π radians

The first and third hypotheses have only implications for the energy state of the folded tape spring. The second hypothesis is also important for being a linear guide, as the motion of the tape loop would not be a perfect straight horizontal line when the fold radius is not constant.

These three hypotheses will be tested using a finite element analysis.

Analysis Metrics. A tape spring is modeled in a FEM model. One of the endpoints is clamped while the other endpoint is rotated π radians to create a single fold. The output of the model is the deformed geometry and the strain energy per surface area within the tape spring.

The deformed geometry is used to find the different regions within the tape spring by analyzing the curvature. The curvature in the undeformed region is zero in longitudinal and constant in transverse direction. In the bent region, this is the opposite. Therefore the different regions can be determined by analyzing the curvature in transverse direction. This is done by curve fitting circles to each transverse line in the longitudinal direction of the tape spring. From these fitted circles the curvature is obtained. When the curvature differs more than 0.1% from the undeformed tape spring radius, the transition region is defined to start. When the curvature is lower than 5% of the original tape spring curvature $\frac{1}{R}$, the start of the bent region is defined.

As the different regions are defined, the length of the transition region can be determined by measuring the length between the start of the transition region and the start of the bent region.

The energy is summed in the transverse direction to see the energy distribution in longitudinal direction. Using the information about the regions, the energy related to each region is summed to get the total energy per region.

The fold radius is determined by fitting a circle to the data points in the bent region in the longitudinal direction.

Finally, the fold angle is determined by calculating the angle between the edges of the bent region and the center of the fitted circle.

TABLE 1. USED VALUES OF TAPE SPRING PARAMETERS.

R	t	L	θ	E	ν
[mm]	[mm]	[mm]	[rad]	[GPa]	[-]
21	0.2	1000	π	210	0.3

Dimensional Design. Within this research, the equal sense bent configuration will be examined. The subtended angle will be varied between 80 and 170 degrees. All other parameters as shown in Fig. 1 are constant as given in Tab. 1.

FEM Analysis. A Matlab based finite element software package of the Delft University of Technology is used for this analysis [19]. The model is based on isogeometric analysis (IGA). Within this framework a geometry is defined using NURBS. The advantage of using this method is that there is no approximation involved in the discretisation of the geometry. The discretisation is realized by refinement of the parametric description of the geometry, which increases the amount of parameters without altering the geometry itself. For a detailed

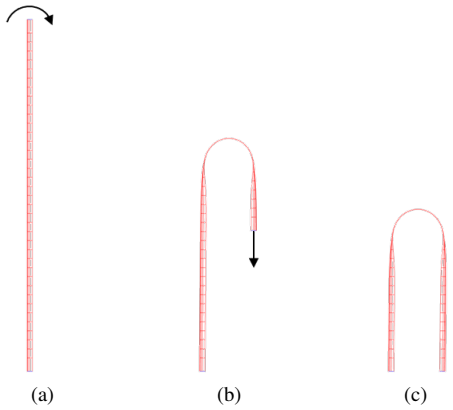

FIGURE 4. FEM STEPS: A) ENDPOINT ROTATION OF π, B) VERTICALLY DISPLACE ENDPOINTS TO SAME HEIGHT, C) FINAL DEFORMED GEOMETRY.

description of the IGA working principle, the reader is referred to [20].

The cross section of the tape spring geometry is defined by an arc with a subtended angle α that is linearly divided into 21 points in the transverse direction. The geometry in the length direction is then defined by linearly spacing these cross sections in longitudinal direction over length L, divided into 300 points. In addition, two so-called pilot points are defined at the centroid of the cross section at both ends of the geometry in longitudinal direction which are connected through beams to each point of the corresponding curved edges. The motions are applied to these pilot points.

The folding process, shown in Fig. 4, is performed in two steps: first a rotation of π is applied to one of the pilot points while the other pilot point is fixed, which forces the tape spring to buckle. Secondly the rotated endpoint is translated to the same height as the fixed pilot point while constraining the rotation.

RESULTS

Not all subtended angles resulted in a converged simulation. The following angles did converge and were included in the analysis

$$\alpha = (85, 90, 95, 100, 105, 110, 115, 120, 125, 140, 145, 155, 160, 165, 170). \quad (3)$$

By analyzing the curvature of the cross sections in transverse direction, the undeformed, transition and bent regions were determined. Figure 5 shows the length of the transition region as function of the subtended angle. It shows that the length of the transition regions increases with the subtended angles.

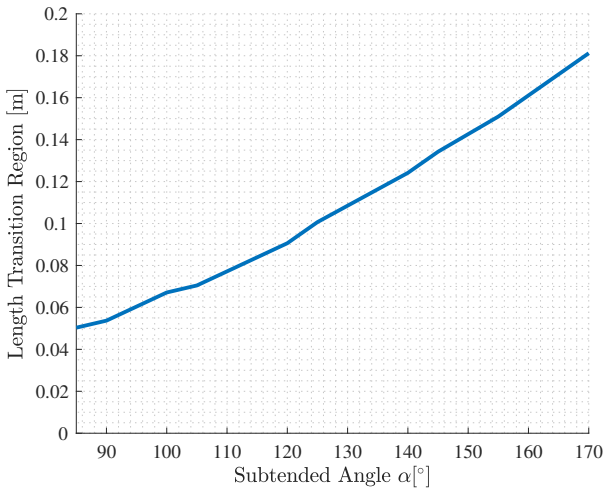

FIGURE 5. LENGTH OF TRANSITION REGIONS FOR DIFFERENT SUBTENDED ANGLES.

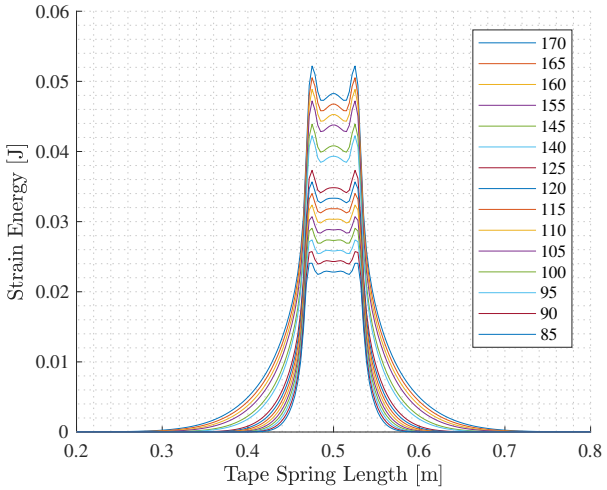

FIGURE 6. ENERGY DISTRIBUTION IN LONGITUDINAL DIRECTION FOR DIFFERENT SUBTENDED ANGLES. THE ORDER OF THE CURVES FROM TOP TO DOWN IS IN THE SAME ORDER AS THE LEGEND. SUBTENDED ANGLES ARE IN DEGREES.

The strain energy is summed in transverse direction to get the energy distribution in longitudinal direction. Figure 6 shows the energy distribution for different subtended angles.

Using the information of the different regions within a tape spring, the energy related to each region could be determined. This energy is summed per region to see the distribution between the different regions, as shown in Fig. 7. The figure shows that a significant part of the total energy is within the transition regions, starting at 25% at a subtended angle of 85 degrees to 45% at a subtended angle of 170 degrees. There is also a small amount of

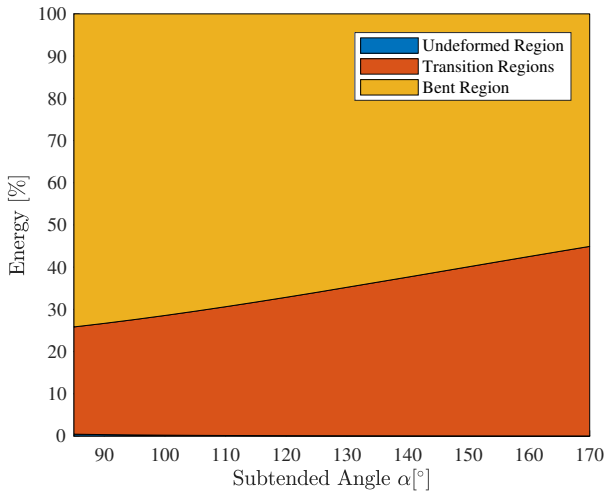

FIGURE 7. PERCENTAGE OF ENERGY PER REGION. NOTE THE SMALL BLUE AREA IN THE LOWER LEFT CORNER.

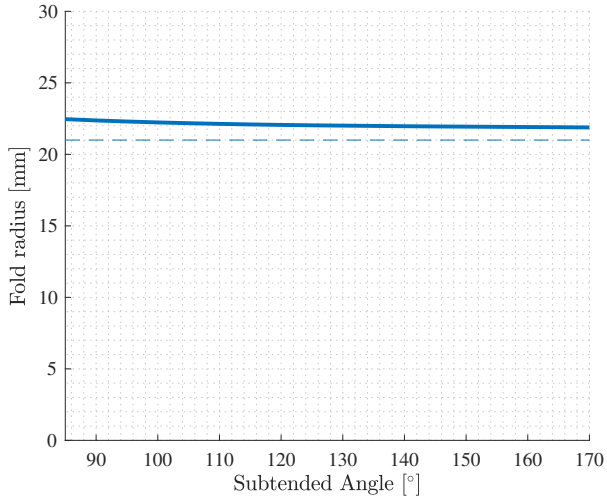

FIGURE 8. FOLD RADII FOR DIFFERENT SUBTENDED ANGLES. DASHED LINE IS THE TAPE SPRING RADIUS.

the energy in the undeformed region at smaller subtended angles.

The fold radius is shown in Fig. 8. The figure shows that fold radius is larger than the tape spring radius, with a mean value 22.1 mm. The maximum difference between the tape spring radius and the fold radius is 7%.

The relation between the fold angle and the subtended angle is shown in Fig. 9. The figure shows that the fold radius is not equal to 180° but varies between varies from 153.6° to 157.7° with a mean value of 156.2°. Figure 10 shows the comparison of the energy within the bent region between the FEM model and the equation using fold angle $\theta = \pi$ and $\theta = 2.73$ $(= 156.2°)$.

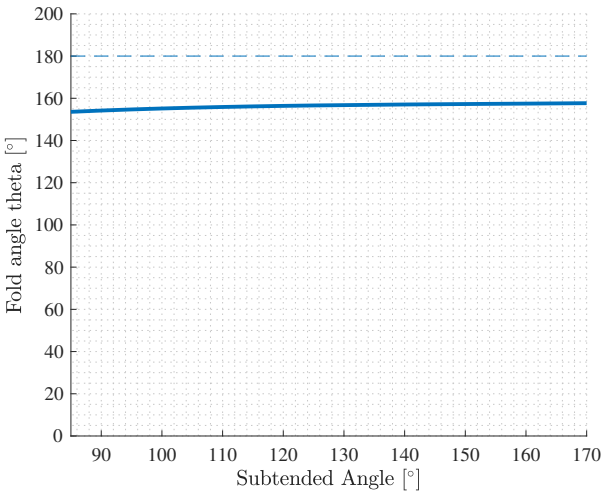

FIGURE 9. FOLD ANGLE FOR DIFFERENT SUBTENDED ANGLES. DASHED LINE IS 180 DEGREES LINE.

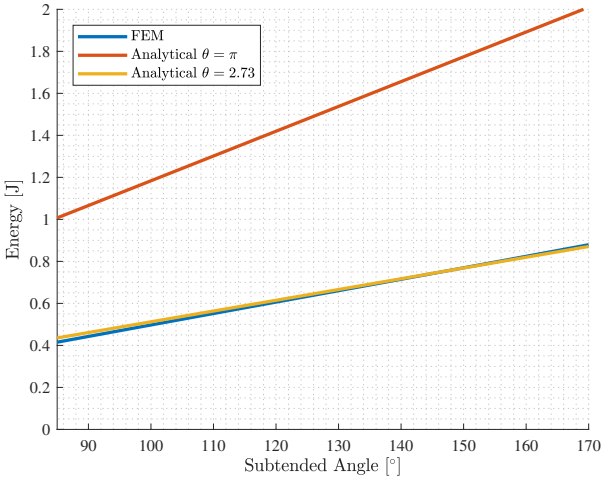

FIGURE 10. ENERGY WITHIN BENT REGION COMPARISON OF FEM AND ANALYTICAL MODEL.

DISCUSSION

It is notable that all of the geometries with a subtended angle below 85 degrees did not results in a converged simulation. This could be caused by the low stiffness due to the small subtended angles of which makes the relatively long structure less stable and therefore hard to solve.

Every curve of the energy distribution plot in longitudinal direction shows two peaks. These peaks seem to match the edge of bent region. From this edge on, the energy content starts to drop. The curvature analysis showed that the curvature in the middle of the bent region is lower than at the edges of the bent regions. This explains the peaks at the edges of the bent regions.

Figure 5 shows discontinuities in the relation between the length of the transition lengths and the subtended angle. These discontinuities can be explained by the way different regions of a tape spring are defined. This is done by calculating the curvature of the transverse lines. The distance between two transverse lines in longitudinal direction is $1\,\mathrm{m}/300 = 0.0033\,\mathrm{m}$, and therefore the length of the transition regions has fixed increments of $0.0033\,\mathrm{m}$.

Figure 7 shows that the energy in the transition zone cannot be neglected. The ratio of the transition and the bent region increases with the subtended angle. At small subtended angles, there is also a small fraction of the energy within the undeformed region. This can be explained by the phenomena that a tape spring start to behave like a flat leaf spring when the subtended angle gets smaller. In a leaf spring, the energy is not concentrated at a fold like in a tape spring, but is evenly distributed in the whole structure.

The fold radius is clearly not the same as the tape spring radius with a maximum difference of 7%. However, when comparing the calculated energy with the actual fold radii using Eqn. (1) and simplified Eqn. (2) where the radii are assumed to be equal, the maximum difference in calculated energy is only 0.32%. This difference is small enough to be neglected.

Furthermore, the fold radius gets larger at small subtended angles. This can be explained by the same phenomena as with the energy distribution. When folding a leaf spring, the smallest energy state of the leaf spring is with the largest radius as possible. Therefore a tape spring with a small subtended angle has a large fold radius. When using a tape spring as a force generator, this results in an imperfect straight line linear guidance. However, when the subtended angle is larger than 100°, the fold radius is fairly constant. So when keeping the subtended angle above this value, a tape loop could be used as a linear force generator.

Figure 9 shows that the fold angle is not equal to 180 degrees, but varies from 153.6 to 157.7 degrees. This is explained by the fact that the curvature of the structure in transverse direction is still not zero, while the structure starts to deform in longitudinal direction. The definition of the bent zone is that it starts when the curvature in transverse direction is zero, so a small part of the fold angle already occurs in the transition regions. This implies that the energy within the bent region of a tape spring fold should be calculated with a value of 2.73 radians $(= 156.2^\circ)$ radians instead π radians.

Figure 10 shows the comparison of the energy within the bent region between the FEM model and the equation using $\theta = \pi$ and $\theta = 2.73$. The figure shows that the line of $\theta = 2.73$ almost perfectly matches the FEM model. At low subtended angles the calculated energy is higher than the FEM model and at high subtended angles, the calculated energy is lower than the FEM. This can be explained by the fact the the fold angle increases with the subtended angle.

CONCLUSION

In this paper, the dependency of the energy distribution within a tape spring on the subtended angle is investigated. Several hypotheses where stated: 1) The energy within the transition regions can be neglected, 2) The fold radius is independent of the subtended angle and equal to the tape spring radius, 3) The fold angle is independent of the subtended angle with a constant value of π radians.

The first hypothesis is rejected, because a significant part of the total energy is within the transition regions. The energy within the transition region as function of the total energy gets even higher at larger subtended angles. The length of the transition zones is dependent on the subtended angle as well.

The second hypothesis is rejected as well. The fold radius gets larger with a smaller subtended angle and is always larger than the tape spring radius. However, the consequences to the total energy state of the tape spring are limited, because the difference in fold radius causes only a difference of 0.32% to the total energy. Therefore this dependency can be neglected for the determination of the total energy. However, for the linear guide, the radius dependency can be a problem. Nonetheless, this problem can be limited by using subtended angles above 100 degrees.

The third and last hypothesis is also rejected. The fold angle is not a constant of 180 degrees, but varies between 153.6 and 157.7 degrees with a mean value of 156.2 degrees. Therefore the fold angle used to calculate the energy within the bent region should be $\theta = 2.73$ radians $(= 156.2^\circ)$. The equation of the energy within the bent region then becomes

$$U_{\text{bent}} = 2.73 \cdot \frac{\alpha E t^3}{12(1 \pm \nu)}. \tag{4}$$

These results imply that the transition regions can not be neglected, but should be incorporated into the synthesis method of a force generator using two-fold tape loops. The subtended angle should preferably be larger than 100 degrees to limit the subtended angle dependency of the fold radius.

REFERENCES

[1] Howell, L. L., Magleby, S. P., and Olsen, B. M., eds., 2013. *Handbook of Compliant Mechanisms*. John Wiley & Sons Ltd., New Delhi, India.

[2] Lamers, A., Sánchez, J. A. G., and Herder, J. L., 2015. "Design of a statically balanced fully compliant grasper". *Mechanismand Machine Theory,* ***92***, pp. 230–239.

[3] Kota, S., Joo, J., Li, Z., Rodgers, S. M., and Sniegowski, J., 2001. "Design of Compliant Mechanisms: Applications to MEMS". *Analog Integrated Circuits and Signal Processing,* ***29***, pp. 7–15.

[4] Radaelli, G., and Herder, J. L., 2017. "Gravity balanced compliant shell mechanisms". *International Journal of Solids and Structures,* ***118-119***, pp. 78–88.
[5] Calladine, C. R., 1988. "The theory of thin shell structures 1888-1988". *Institution of Mechanical Engineers,* ***202***(A3), pp. 141–149.
[6] Seffen, K. A., and Pellegrino, S., 1999. "Deployment dynamics of tape springs". *The Royal Society,* ***455***, pp. 1003–1048.
[7] Soykasap, Ö., 2007. "Analysis of tape spring hinges". *International Journal of Mechanical Sciences,* ***49***, pp. 853–860.
[8] Seffen, K. A., Pellegrino, S., and Parks, G. T., 2000. "Deployment of a Panel by Tape-Spring Hinges". In IUTAM-IASS Symposium on Deployable Structures: Theory and Applications, Kluwer Academic Publishers, pp. 355–364.
[9] Vehar, C., Kota, S., and Dennis, R., 2004. "Closed-Loop Tape Springs as Fully Compliant Mechanisms : Preliminary Investigations". In 28th Biennial Mechanisms and Robotics Conference, ASME, pp. 1–10.
[10] Houwers, H., 2016. "Closed-Loop Two-Fold Tape Spring Transmissions". Master thesis, Delft University of Technology.
[11] NASA, 1967. Rolamite: New Mechanical Design Concept. Tech. Rep. 67-10611, NASA, Springfield, Virginia.
[12] Cadman, R. V., 1970. Rolamite - Geometry and Force Analysis. Tech. rep., Sandia Laboratories, Albuquerque, N. Mex.
[13] English, C., and Russell, D., 1999. "Implementation of variable joint stiffness through antagonistic actuation using rolamite springs". *Mechanism and Machine Theory,* ***34***, pp. 27–40.
[14] Radaelli, G., 2017. "Synthesis of Mechanisms with Prescribed Elastic Load-Displacement Characteristics". Phd thesis, Delft University of Technology.
[15] Bourgeois, S., Cochelin, B., Guinot, F., and Picault, E., 2012. "Buckling analysis of tape springs using a rod model with flexible cross-sections". *European Journal of Computational Mechanics,* ***21***(3-6), pp. 184–194.
[16] Walker, S. J. I., and Aglietti, G. S., 2007. "A study of tape spring fold curvature for space deployable structures". In IMechE Vol. 221 Part G: J. Aerospace Engineering, IMechE, pp. 313–325.
[17] Seffen, K. A., 2001. "On the Behavior of Folded Tape-Springs". *Journal of Applied Mechanics,* ***68***, pp. 369–375.
[18] Calladine, C. R., 1983. *Theory of Shell Structures*. Cambridge University Press, New York.
[19] Radaelli, G., and Herder, J. L., 2016. "Shape optimization and sensitivity of compliant beams for prescribed load-displacement response". *Mechanical Sciences,* ***7***, pp. 219–232.
[20] Cottrell, J. A., Hughes, T. J. R., and Bazilevs, Y., 2009. *Isogeometric Analysis: Toward Integration of CAD and FEA*. John Wiley & Sons, Ltd, Chichester.

4

Paper: Synthesis of a Force Generator with Custom Force Displacement Behavior Using Two-Fold Tape Loops

SYNTHESIS OF A FORCE GENERATOR WITH CUSTOM FORCE DISPLACEMENT BEHAVIOR USING TWO-FOLD TAPE LOOPS

Marinus G. de Jong
Dept. of Precision and Microsystems Engineering
Delft University of Technology
Delft, 2628 CD, The Netherlands
Email: M.G.deJong@tudelft.nl

Werner W.P.J. van de Sande
Just L. Herder
Dept. of Precision and Microsystems Engineering
Delft University of Technology
Delft, 2628 CD, The Netherlands
W.W.P.J.vandeSande@tudelft.nl, J.L.Herder@tudelft.nl

ABSTRACT

Tape springs are thin-walled structures with zero longitudinal and constant transverse curvature. Folding them twice and connecting both ends creates a tape loop. A tape loop can act as a zero stiffness linear guide when using a constant cross-section. If a tape spring with a non-constant cross-section is used, the total energy state of the tape loop differs at different positions, so a force generator can be created.

A synthesis method is developed to determine the required geometry for obtaining the desired force displacement behavior. Fifteen force displacement curves are defined which all describe a characteristic behavior. These fifteen force displacement curves are used as input to synthesize fifteen tape spring geometries. The resulting geometries are simulated in a finite element model to validate the synthesis method. The geometry with a non-zero constant force characteristic, is optimized, produced and tested in an experiment.

All fifteen force displacement behaviors could be approximated by the synthesized geometries. The optimized design succeeded to obtain the required force displacement behavior. The experiment showed that the produced tape spring with a constant cross-section has already irregularities in its force displacement. When it was cut to the synthesized geometry, this resulted in a shift of the force displacement curve.

In conclusion, a tape loop can act as an all-purpose force generator using the developed synthesis method. However, before practical application, several production challenges need to be overcome.

INTRODUCTION

Tape springs are thin-walled structures with zero longitudinal and constant transverse curvature. A carpenters tape is an example of such geometry. Despite its simple geometry, a tape spring has some remarkable properties, such as being stiff before buckling while being compliant after buckling, having a constant fold radius [1] and constant moment after buckling [2]. Because of these properties, tape springs are used as hinges [3] or deployable stiff structures in space [4].

By making multiple folds and connecting both ends, a tape loop is created. Vehar [5] examined different setups with a different number of folds. A tape loop with two folds is the simplest configuration, which acts as a zero force and zero stiffness linear guide as explored by Houwers [6].

A mechanism that has a similar working principle as a two-fold tape loop is a rolamite [7]. A rolamite can act as force generator by changing the geometry of the band [8, 9]. In further analogy to the rolamite, a tape loop can be turned into a force generator by changing the cross section of the tape spring. In this way a monolithic equivalent of the rolamite is obtained. One of the advantages of using a tape loop as a force generator is that because of its monolithic geometry, it is theoretically highly scalable, especially for smaller scales. This makes it for example interesting for minimally invasive surgery by using a nearly constant force mechanism using a two-fold tape loop with a tapered tape spring as suggested by Radaelli [10].

De Jong [11] (chapter three of this thesis) has shown that both the length of the transition regions and the energy within the transition regions as ratio of the total energy increases with higher subtended angles. Another observation was that the fold radius and angle are influenced by the cross section. This effect is limited when the subtended angle is above 100 degrees.

Within this paper, a synthesis method is developed to synthesize a force generators using two-fold tape loops. The synthesis method consist of an analytical model with the desired force displacement behavior as its input. The model is used to synthesize fifteen different tape spring geometries that all describe a unique force displacement behavior. All these fifteen geometries are modeled in a finite element model to validate their force displacement behavior. The geometry with non-zero constant force behavior is investigated more in-depth and is tested in an experiment.

This paper starts with the basic theory of a folded tape spring. Then the synthesis method of a tape loop and the experiment are explained. The results of the synthesis method and the experiment are presented. In the discussion, the results of the synthesis method and experiment are interpreted. Finally the paper concludes with some remarks.

METHOD

In this section, the synthesis method of a force generator using folded tape springs is explained. It starts by explaining the basics of a tape spring. Then the synthesize method is presented. Fifteen different force displacement curves are presented, which are used to synthesize fifteen tape loop geometries. The section ends with explaining the detailed synthesis and experiment.

Tape Spring Basics

Parameters of a Folded Tape Spring. A tape spring fold is created by applying a moment to both ends of a tape spring. Figure 1 shows an equal sense folded tape spring together with its undeformed geometry. The original geometry has a constant transverse radius R and zero longitudinal radius with a so-called subtended angle α, thickness t and length L. From now on the transverse radius will be called the tape spring radius. The folded geometry has a fold radius R^* with a fold angle θ.

There is some discussion whether the fold radius is equal to the tape spring radius [1,4]. De Jong [11] concluded that the fold radius is larger than the tape spring radius with a maximum of 7% when keeping the subtended angle above 100°. This difference in radius results in a difference in energy state less than 0.5%. The fold radius is hard to determine so for the reason of simplicity, the fold radius is assumed to be equal to the tape spring radius, $R^* = R$.

Tape Spring Regions. Three different regions can be identified within a folded tape spring. Figure 2 shows a folded tape spring with the different regions numbered.

The first region is the undeformed region. This is where the tape spring has its original shape. The second region is called the transition region. In this region the tape spring goes from the original to fully deformed shape. The third region is called the bent region. In this region the tape spring is fully deformed in both transverse and longitudinal direction.

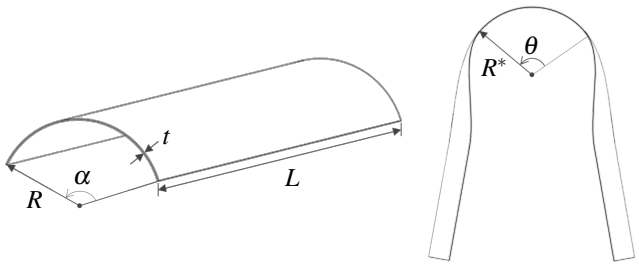

(a) Undeformed tape spring (b) Folded tape spring

FIGURE 1. PARAMETERS OF AN EQUAL SENSE FOLDED TAPE SPRING.

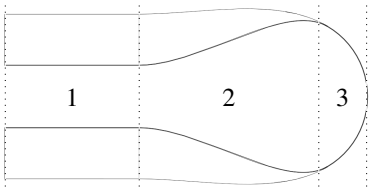

FIGURE 2. DIFFERENT REGIONS WITHIN A FOLDED TAPE SPRING: 1) UNDEFORMED REGION, 2) TRANSITION REGION, 3) BENT REGION.

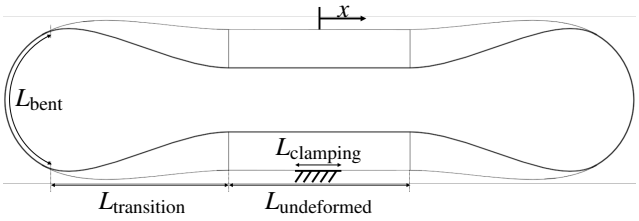

FIGURE 3. TWO-FOLD TAPE LOOP.

Tape Loop. By folding a tape spring twice and connecting both sides, a two-fold tape loop is created. The motion is applied to the upper side of the loop while the lower side is clamped, as shown in Fig. 3.

Using a tape spring in the two-fold tape loop configuration has two implications for the parameters: 1) the folding angle θ is π radians, 2) the subtended angle α can have a maximum value of π radians, because otherwise the two sides of the tape loop would collide.

Range of Motion. When the transition region hits the clamping, the part of the tape spring at the edge of the clamping

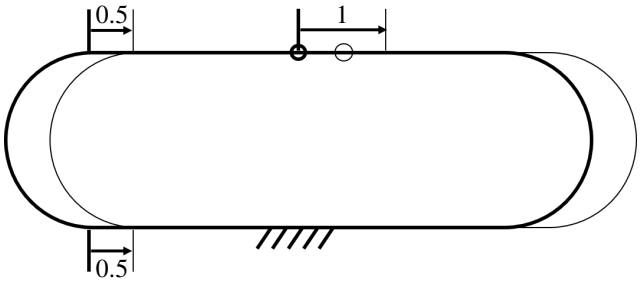

FIGURE 4. ILLUSTRATION OF THE RANGE OF MOTION. THICK LINE IS ORIGINAL POSITION, THIN LINE THE POSITION AFTER THE DISPLACEMENT. THE CIRCLES INDICATE THE MIDDLE OF THE TAPE LOOP.

wants to flatten in transverse direction. This flattening is however restricted by the clamping. This results in a high stiffness in the direction of the motion, which limits the range of motion (ROM).

The length of the motion without this stiffening effect is determined by the length of the undeformed region at the side of the clamping. This length is the total undeformed length divided by two minus the length of the clamping

$$\begin{aligned} L_{\text{undef,lower}} &= \frac{L_{\text{undef}}}{2} - L_{\text{clamping}} \\ &= \frac{L - 2\cdot L_{\text{bent}} - 4\cdot L_{\text{trans}}}{2} - L_{\text{clamping}} \\ &= \frac{L - 2\cdot(\pi R) - 4\cdot L_{\text{trans}}}{2} - L_{\text{clamping}} \\ &= \frac{L}{2} - \pi R - 2\cdot L_{\text{trans}} - L_{\text{clamping}} \end{aligned} \tag{1}$$

When a motion is applied to the tape loop, the whole structure shifts in that direction. However, the point at which the motion is applied rolls to that direction as well. Figure 4 shows an example to illustrate this behavior. Because of this behavior, the ROM is twice the length of the undeformed region at the lower side

$$\text{ROM} = 2\cdot L_{\text{undef,lower}} \tag{2}$$

Equation of Energy. De Jong [11] suggested that the strain energy in the bent region of a single equal sense folded tape spring can be approached by

$$U = 2.73\cdot\frac{\alpha E t^3}{12(1+\nu)} \tag{3}$$

In that research, the subtended angle remained constant over the length of the tape spring. In this paper however, the subtended angle will not be constant but it will have a profile. The subtended angle α is therefore not a constant value, but is the average subtended angle in the bent. Furthermore, there are two folds in a tape loop, so when the profile of the cross section is equal for both folds, the energy is twice the energy of a single fold. These additions result in

$$U = 2.73\cdot\frac{\overline{\alpha}_{\text{bent}} E t^3}{6(1+\nu)} \tag{4}$$

Relation Between Radius and Thickness. The von Mises principal plane stress is given by

$$\sigma_v = \sqrt{\sigma_1^2 - \sigma_1\sigma_2 + \sigma_2^2}. \tag{5}$$

Using Kirchhoff-Love plate theory for an isotropic and homogeneous plate without shear strain, $\vec{\sigma}$ is given by

$$\vec{\sigma} = \begin{bmatrix}\sigma_1\\ \sigma_2\end{bmatrix} = \frac{E}{1-\nu^2}\begin{bmatrix}1 & \nu\\ \nu & 1\end{bmatrix}\vec{\varepsilon}_{\text{max}} \tag{6}$$

where $\vec{\varepsilon}_{\text{max}}$ is the maximum strain. In case of an equal sense folded tape spring, the maximum strain in longitudinal direction is $\varepsilon_1 = t/2R$ and in transverse direction $\varepsilon_2 = -t/2R$. Substituting these values in Eqn. (5) and (6) results in an expression of the von Mises stress

$$\sigma_v = \frac{Et\sqrt{3}}{2R(1+\nu)}. \tag{7}$$

This expression shows that the von Mises stress increases with the thickness and decreases with the radius. According to the von Mises yield criterion, a material starts to yield when the von Mises stress reaches the yield strength of a material, so $\sigma_v < \sigma_y$ to prevent plastic deformation. Using this criterion, Eqn. (7) can be rearranged to obtain the relation between t and R

$$t < \frac{2\sigma_y(1+\nu)}{E\sqrt{3}}R. \tag{8}$$

Maximum Energy. Substitution of Eqn. (8) into Eqn. (4) with the maximum average subtended angle of π results in the maximum energy that can be stored in a tape loop as function of the material parameters and radius

$$U_{\text{max}} = 2.73\cdot\frac{4\pi}{9\sqrt{3}}\cdot\frac{\sigma_y^3(1+\nu)^2}{E^2}\cdot R^3 \tag{9}$$

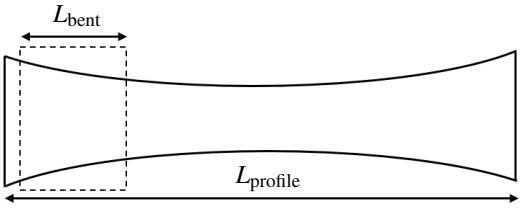

FIGURE 5. SCHEMATIC REPRESENTATION OF THE TOP VIEW OF AN UNFOLDED TAPE SPRING WITH SUBTENDED ANGLE PROFILE.

Using this equation, the von Mises stresses will be just as high as the yield stresses. In practice, a safety factor should be incorporated to prevent plastic deformation.

Maximum Force. The force exerted by the tape loop is the difference in energy divided by its displacement. Theoretically, a tape loop can go from maximum energy ($\overline{\alpha} = \pi$ radians) to zero energy ($\overline{\alpha} = 0$ radians) in a displacement of two times the arc length of the bent πR, when only taking the energy within the bent region into account. Note that the displacement is twice the arc length of the bent because of the same phenomena as illustrated in Fig. 4. The theoretical maximum force is therefore

$$\begin{aligned} F_{\text{max,theoretical}} &= \frac{U(\pi) - U(0)}{2\pi R} \\ &= 2.73 \cdot \frac{2}{9\sqrt{3}} \cdot \frac{\sigma_y^3 (1+\nu)^2}{E^2} \cdot R^2. \end{aligned} \tag{10}$$

However, in [11] the lower boundary of $\pi/2$ radians for the subtended angle is given to prevent undesired behavior. This results in the maximum force

$$\begin{aligned} F_{\text{max}} &= \frac{U(\pi) - U(\pi/2)}{2\pi R} \\ &= 2.73 \cdot \frac{1}{9\sqrt{3}} \cdot \frac{\sigma_y^3 (1+\nu)^2}{E^2} \cdot R^2. \end{aligned} \tag{11}$$

Range of Desired Behavior. Besides the physical range of motion, there is a limited range where the tape loop can generate the desired force. Figure 5 shows a schematic representation of the top view of an unfolded tape spring profile. The dashed box shows the part of the tape spring that is in the bent when the tape spring is folded. The maximum shift of the bent to the right is the total length of the profile L_{profile} minus the arc length of the bent L_{bent}. Because of the same phenomena as explained at the range of motion section, this length is multiplied by two

$$\begin{aligned} \text{RODB} &= 2\left(L_{\text{profile}} - L_{\text{bent}}\right) \\ &= 2\left(L_{\text{profile}} - \pi R\right) \end{aligned} \tag{12}$$

This means for example that there is zero range of desired behavior when the length of the profile is the same as the arc length.

Synthesis Method.

De Jong [11] showed that a significant part of the strain energy is stored in the transition zones and that it does not scale linearly with increasing subtended angles. The description of the energy within the transition regions is therefore complex. For the reason of this complexity, the synthesis method will first be simplified by taking only the energy in the bent region into account. The next step is performing a more in depth analysis, to compensate the error involved in this simplification. Because the force exerted is calculated by the difference in strain energy, the error involved in this simplification is limited to the difference of the strain energy in the transition regions.

The synthesis method consists of three steps

1. Obtain average subtended angle from desired force displacement behavior, given as numerical polynomial
2. Construct average subtended angle polynomial from subtended angle polynomial with parametric coefficients
3. Solve coefficients of the parametric subtended angle polynomial using the numerical polynomial of the average subtended angle

The synthesis method starts by defining the desired force equation as a polynomial

$$F(x) = \sum_{k=0}^{n} a_k x^k, \tag{13}$$

where the coefficients a_k are real numeric values, based on the desired force displacement behavior. The strain energy is obtained by integrating the force equation

$$\begin{aligned} U(x) &= \int F(x) \\ &= \sum_{k=0}^{n} \frac{a_k}{k+1} x^{k+1} + C. \end{aligned} \tag{14}$$

The expression of the strain energy of Eqn. (4) can now be substituted into Eqn. (14). After some rearranging, the following

expression for the average subtended angle is obtained

$$\overline{\alpha}_{\text{bent}}(x) = \frac{6(1+\nu)}{2.73 \cdot Et^3} \sum_{k=0}^{n} \frac{a_k}{k+1} x^{k+1} + C \tag{15}$$

The second step is to define the cross-section profile as a polynomial, but with parametric coefficients

$$\alpha(x) = \sum_{k=0}^{n} b_k x^k \tag{16}$$

The average subtended angle over the bent length $R\theta$, is calculated by integrating Eqn. (16) with the boundaries x and $x+\beta$, divided by β, where β is the arc length of the bent $R\theta$

$$\begin{aligned} \overline{\alpha}_{\text{bent}}(x) &= \frac{1}{\beta} \int_{x}^{x+\beta} \alpha(x) dx \\ &= \frac{1}{\beta} \sum_{k=0}^{n} \frac{b_k}{k+1} \left[(x+\beta)^{k+1} - (x)^{k+1} \right] \end{aligned} \tag{17}$$

The third step is solving Eqn. (17) using Eqn. (15), which results in the unknown values of the parametric polynomial coefficients b_k of the geometry equation. Constant C is still unknown. This constant is introduced in Eqn. (14) at the integration of the required force to obtain the required strain energy. Constant C therefore determines the base energy level of the tape spring. The value of this constant is given by constraining the minimum subtended angle to 100 degrees, as advised by [11].

Force Displacement Curves. In the chapter two, fifteen unique force displacement curves were defined to quantify the level of customizability of a force generator with custom force displacement behavior. These fifteen curves are used as input of the synthesis method for two purposes: 1) To verify whether the synthesis method can be used to attain geometries with the desired force displacement behavior and 2) to verify whether a two-fold tape loop can be used as an all-purpose force generator.

The polynomial input force displacement curve of Eqn. (13) is constructed by defining the required force at the start, the middle and the end of the motion. A polynomial is fitted through these data points. Table 1 gives an overview of the data points together with its polynomials used for constructing the required force curves. The synthesis method is based on two tape spring folds. For this analysis, a single fold will be used, so Eqn. (15) is multiplied by two.

The performance of the synthesis method is verified by simulating the resulting geometries in a finite element model. The force displacement behavior of the simulated geometries is compared with the force displacement curve given as input of the synthesis model. This comparison is done by performing a least-squares polynomial fit through the simulated data, with polynomials that have the same order as the original force displacement curves. For example in case of function number 1, the equation of the polynomial fit is constructed by a quadratic term and a constant, i.e. $c_1 x^2 + c_2$. The norm of the residuals gives an indication on how well the simulated data can be described by a polynomial with the same order as the original polynomial.

TABLE 1. DATA USED FOR CONSTRUCTING THE FORCE FUNCTIONS

Function Nr	Datapoints [N]	Force Polynomial [N]
1	(0.2, 0.4, 1.0)	$\frac{5}{4}x^2 + \frac{1}{5}$
2	(0.2, 0.6, 1.0)	$x + \frac{1}{5}$
3	(0.2, 0.8, 1.0)	$-\frac{5}{4}x^2 + 2x + \frac{1}{5}$
4	(-0.4,-0.2, 0.4)	$\frac{5}{4}x^2 - \frac{2}{5}$
5	(-0.4, 0.0, 0.4)	$x - \frac{2}{5}$
6	(1.0, 0.5, 1.0)	$\frac{25}{8}x^2 - \frac{5}{2}x + 1$
7	(0.6, 0.6, 0.6)	$\frac{3}{5}$
8	(0.5, 1.0, 0.5)	$-\frac{25}{8}x^2 + \frac{5}{2}x + \frac{1}{2}$
9	(0.5, 0.0, 0.5)	$\frac{25}{8}x^2 - \frac{5}{2}x + \frac{1}{2}$
10	(0.0, 0.0, 0.0)	0
11	(1.0, 0.4, 0.2)	$\frac{5}{4}x^2 - 2x + 1$
12	(1.0, 0.6, 0.2)	$-x + 1$
13	(1.0, 0.8, 0.2)	$-\frac{5}{4}x^2 + 1$
14	(0.4,-0.2,-0.4)	$\frac{5}{4}x^2 - 2x + \frac{2}{5}$
15	(0.4, 0.0,-0.4)	$-x + \frac{2}{5}$

Detailed Synthesis. The synthesis method only takes the energy in the bent region into account, while a significant part of the energy however is stored in the transition regions. Therefore the actual force displacement behavior will not exactly match the desired force displacement behavior. To illustrated that the force displacement behavior can be tuned to match the requirements, the geometry with non-zero constant force behavior (function number 7) is synthesized in more detail. The constant force behavior is chosen because Radaelli [10] proposed a constant force mechanism with a tapered cross-section, while the FEM analysis in Radaelli's research showed that a tapered ge-

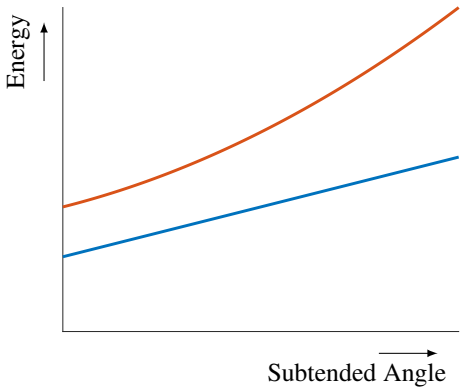

FIGURE 6. ILLUSTRATION OF ENERGY DISTRIBUTION FOR DIFFERENT SUBTENDED ANGLES. BLUE IS ENERGY IN BENT REGION, RED IS ENERGY IN BENT REGION PLUS ENERGY IN TRANSITION REGION

ometry results in a small stiffness.

This stiffness can be explained by the fact that while the energy in the bent region scales linearly with the subtended angle, the energy in the transition region scales progressively. Therefore the total energy state of the tape loop does not scale linear with the subtended angle but it increases progressively, which is illustrated in Fig. 6.

In order to obtain constant force behavior, i.e. the energy in-/decreases linearly, the geometry should compensate the progressive increasing energy curve. Therefore several geometries with a digressive increasing geometries were synthesized. The geometries were defined by three points, which are located at the start, middle and end of the tape spring. The starting and ending point are respectively the minimum and maximum subtended angle, with values of 100 and 145 degrees. The middle point is defined as the average of these angles times a factor $(1+\eta)$

$$\alpha\left(\frac{L}{2}\right) = (1+\eta)\cdot\left(\frac{\alpha(0)+\alpha(L)}{2}\right) \tag{18}$$

where the tape spring's length $L = 1\,\mathrm{m}$ and η are values between 0 (linear line) and 0.1 with increments of 0.02. By fitting a second order polynomial trough these points, the geometries as shown in Fig. 7 are obtained.

Experimental Method.

Tape Spring Production A tape spring is produced from spring steel (1.4310) according to the characteristics shown in Tab. 2. The detailed synthesized geometry is used for the experiment. The profile of the subtended angle is cut out with a laser cutter.

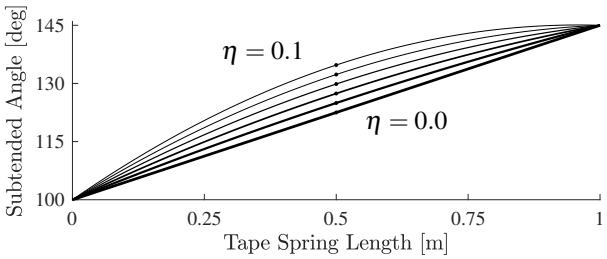

FIGURE 7. GEOMETRIES FOR OBTAINING CONSTANT FORCE BEHAVIOR. THE DOTS INDICATE MIDPOINT OF TAPE SPRING. EACH LINE IS INCREMENTED WITH $\eta = 0.02$.

TABLE 2. TAPE SPRING CHARACTERISTICS OF PRODUCED TAPE SPRING.

R	t	L	α	E	ν	σ
[mm]	[mm]	[mm]	[°]	[GPa]	[-]	[MPa]
26	0.2	1000	150	210	0.3	1600-1800

Measurement Setup. A single fold tape spring is tested on a universal testing machine Z005 of Zwick/Roell. The testing machine makes a vertical translation while measuring the force in the same direction. One end of the tape spring is clamped at the load sensor, which is on the moving part of the machine. The other end is clamped at an aluminum profile which is clamped to the ground. The measurement setup is shown in Fig. 8.

During motion, the length and therefore the weight beneath the load sensor changes. Therefore the measurements are compensated for the gravity by setting the load to zero at the start of the measurement and subtracting the gravity

$$\begin{aligned} F_z &= V\cdot\rho\cdot g \\ &= \left(Rt\int_{L_{\mathrm{start}}}^{L_{\mathrm{start}}+x/2}\alpha(L)dL\right)\cdot\rho\cdot g \end{aligned} \tag{19}$$

, where L_{start} is the length of the tape spring that is already under the load sensor when the load is set to zero.

Measurement Scheme. Four different measurements are performed:

1. **Baseline measurement one:** To investigate the force displacement profile of the produced tape spring itself. The measurement is performed with a tape spring without the subtended angle profile cut out. The load sensor is set to zero at the start of the experiment.
2. **Baseline measurement two:** To investigate the influence of the measurement setup, the same measurement is performed

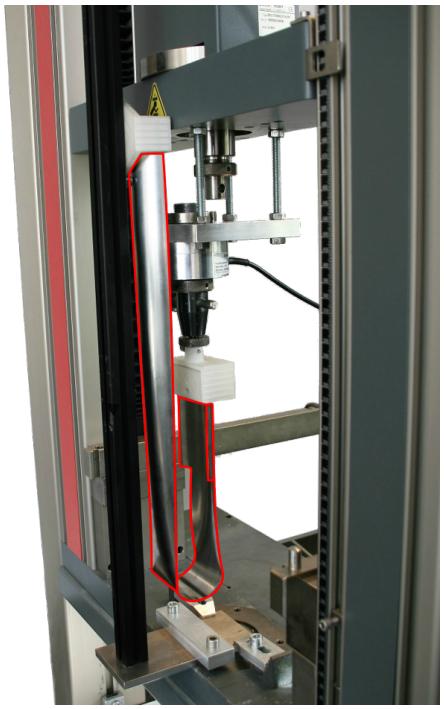

FIGURE 8. MEASUREMENT SETUP. RED DELINEATED STRUCTURE IS FOLDED TAPE SPRING.

with another tape spring. Another goal of performing the experiment with two tape springs is to pick the best performing tape spring for cutting out the profile. The load sensor is set to zero at the start of the experiment.

3. **Curved measurement:** Measurement with the subtended angle profile cut out. The load sensor is set to zero at the start of the experiment.
4. **Curved upside down measurement:** Because the load sensor is set to zero at the start of the experiment with the curved geometry, the force generated due to the subtended angle profile cannot be measured. Therefore a second measurement is performed where the tape spring is rotated 180 degrees, without setting the load sensor to zero again. When there is a force generated by the tape spring, this will result in twice the force in the other direction.

All experiments are repeated five times and averaged to filter out random noise.

RESULTS

Synthesis of Profiles.

The comparison between the desired force displacement behavior and the force displacement behavior according to the FEM simulation of the fifteen synthesized geometries is shown in Fig. 9. All of the curves FEM model follow roughly the curves of the analytical model. Some of the functions show that the force suddenly increases at the end of the displacement. This increasement is most clearly visible at function numbers 3, 8 and 13.

Although all FEM force displacement curves follow roughly the analytical curves, function number 7 does not succeed to obtain the right force displacement characteristic. Function number 7 should have a constant force and zero stiffness, yet it shows that the force is increasing, i.e. the stiffness is not zero.

This observation is confirmed by Fig. 10, which displays the norm of the residuals of the fitted polynomials, normalized to the maximum value. This figure shows also that function number 2, 12 and 13 have higher residual norm than other function numbers.

Detailed synthesis.

Figure 11 shows the force displacement curves of the detailed synthesis of function number 7. It shows that when $\eta = 0.00$, there is a positive stiffness. When $\eta = 0.02$, the force is nearly constant between a displacement of 0.25 m and 0.75 m. The mean force between these displacements is 0.45 N with a maximum difference of 1.8%. When η is larger than 0.02, the stiffness becomes negative. When the values of η are getting higher, the curve gets more bent.

Another observation is that there is a large stiffness at the beginning and end of the displacement, regardless of the value of η.

Experiment.

The resulting force displacement curves of the baseline measurements are shown in figure 12. The shaded areas represent the data points of all five measurements. It shows that the measurements are repeatable, because these shaded areas are small. The measurement also shows that there is a significant amount of hysteresis in the tape springs, which is the largest in the second tape spring. Both tape springs show many irregularities. Both tape springs show large peaks around 0.48 m and 0.58 m. The first tape spring has less peaks and less hysteresis and is therefore used for the other experiments.

Figure 13 shows the measurements of the tape springs with the subtended angle profiles cut out. The figure shows that these measurements are repeatable as well. The black dashed line is the mean line of the both average hysteresis lines. The average value of this line is 0.46 N. This line is the line where the two curves are mirrored, and therefore it represents where the x-axis should be.

Figure 14 shows the curved line, shifted so that the average line matches the x-axis. The hysteresis of this curve is 53 %.

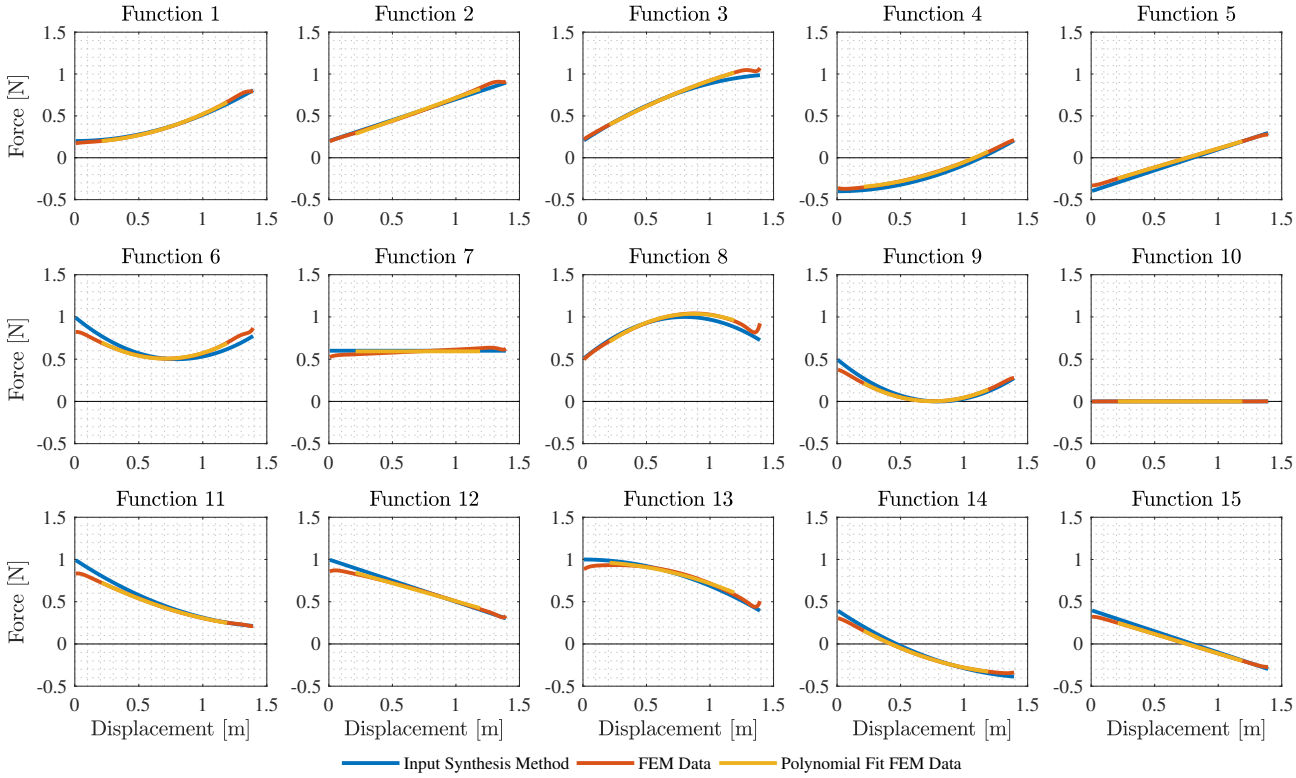

FIGURE 9. FORCE DISPLACEMENT CURVES OF SYNTHESIZED TAPE SPRING PROFILES.

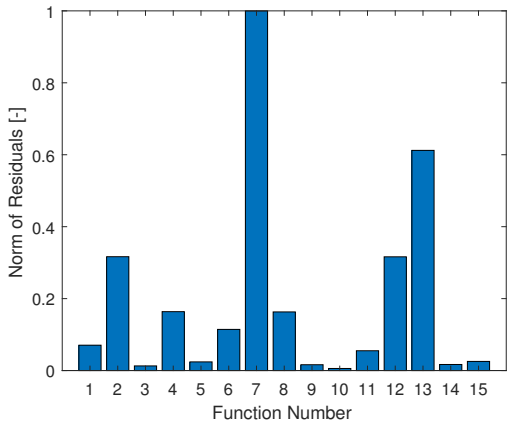

FIGURE 10. NORM OF RESIDUALS OF FITTED POLYNOMIALS. VALUES ARE NORMALIZED TO THE MAXIMUM VALUE.

DISCUSSION

Force Displacement Curves.

The stiffening at the start and end of the displacement is caused by the transition regions that reach the clamping. The tape spring wants to flatten in transverse direction, which is prevented by the clamping. This results in a high stiffness.

Function number 7 has the largest norm of the residuals. This is because the force displacement behavior of this geometry increases, while the desired force displacement behavior is a constant. The resulting force displacement curve is therefore one order higher than desired. The reason for this behavior can be explained by the fact that the energy within the transition region scales progressively with the subtended angle. With a linear increasing subtended angle profile, this results in a progressively increasing energy profile and therefore a stiffness is induced.

Function number 13 has the second highest norm of the residuals. This is because there is no proportional term in the desired force function. When the proportional term is added to the force function, the norm of the residuals is lower than 0.1. The force displacement curve however is still progressively decreasing, so the desired force displacement behavior can be obtained using the synthesis method.

Function number 2 and 12 have the third highest norm of the residuals. Both of these function show a curved line instead of a linear in-/decreasing force displacement curve. The resulting force displacement behavior is therefore, just as function number 7, an order higher than the input force displacement curve. The norm of the residuals of function number 2 and 12 is however three times smaller than the norm of the residuals of number function, so this behavior is less significant.

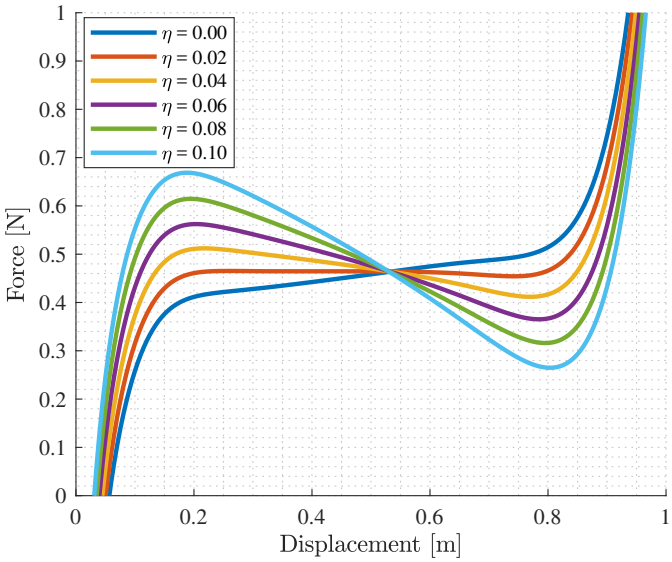

FIGURE 11. FORCE DISPLACEMENT CURVES OF DETAILED SYNTHESIS FOR DIFFERENT VALUES OF η.

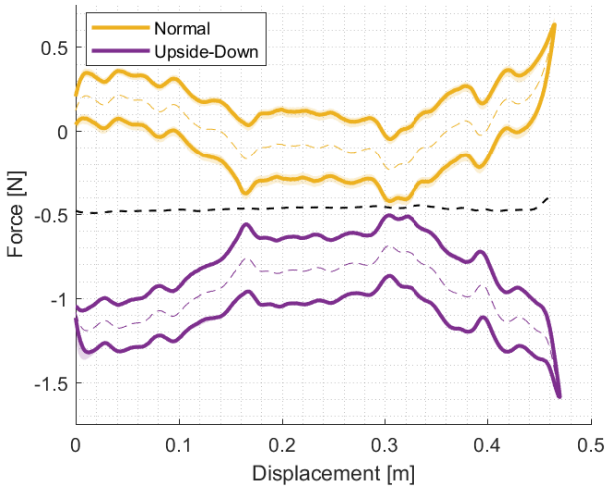

FIGURE 13. MEASUREMENT OF CURVED TAPE SPRING. SHADED AREA IS DATA OF DIFFERENT MEASUREMENTS. COLORED DASHED LINE IS MEAN VALUE OF HYSTERESIS LOOP. BLACK DASHED LINE IS MEAN VALUE OF BOTH LOOPS.

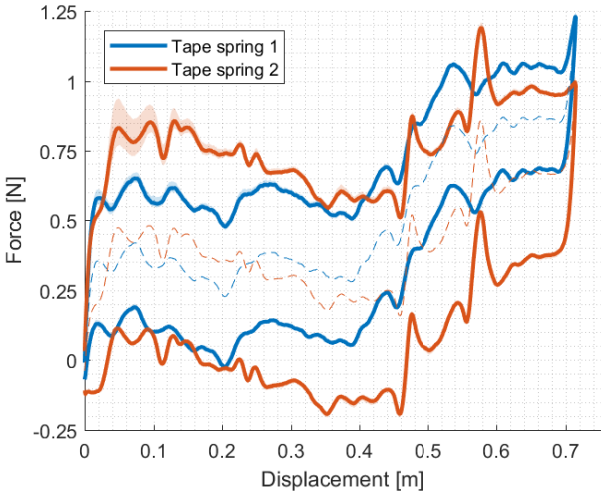

FIGURE 12. BASELINE MEASUREMENTS OF TWO DIFFERENT TAPE SPRINGS. SHADED AREA IS DATA OF DIFFERENT MEASUREMENTS. DASHED LINE IS MEAN VALUE OF HYSTERESIS LOOP.

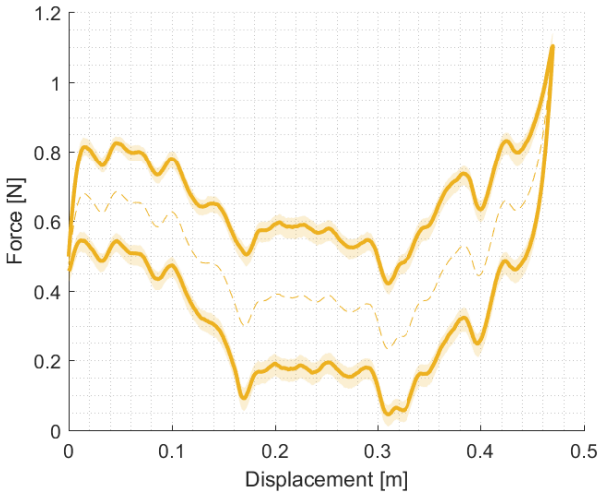

FIGURE 14. MEASUREMENT OF CURVED TAPE SPRING, SHIFTED TO RIGHT HEIGHT. SHADED AREA IS DATA OF DIFFERENT MEASUREMENTS. COLORED DASHED LINE IS MEAN VALUE OF HYSTERESIS LOOP.

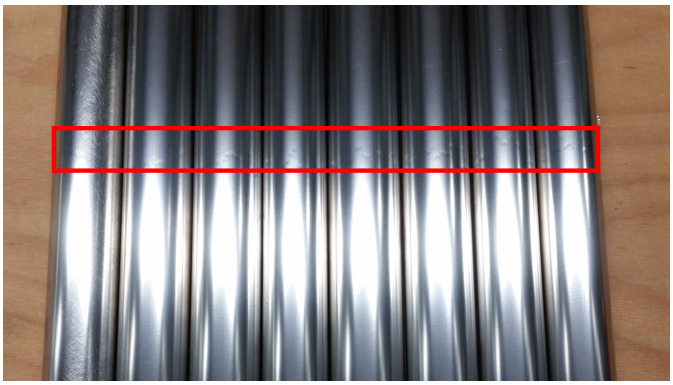

FIGURE 15. CLOSE UP OF PRODUCED TAPE SPRING. RED BORDER SHOWS DENTS IN MIDDLE OF TAPE SPRINGS.

Detailed synthesis.

By using a higher order polynomial than the linear curve of function number 7, a more constant force-displacement curve is obtained. At higher values of η, the stiffness becomes negative, just as in function number 12. This makes sense, because the function then become the same as the geometry of function number 12, which is also has negative stiffness behavior.

Experiment.

The base line measurement was performed with a tape spring with a constant subtended angle and therefore it should have a zero force displacement curvature. The experiment however showed a curve with a lot of irregularities. In order to understand these peaks, the production process of the tape springs will be explained.

Ideally the tape spring would be rolled to get a constant curvature in transverse direction. The yield strength of the spring steel however was too high, which resulted in a large spring back and a radius of 100 mm instead of 21 mm. To obtain a smaller tape spring radius, the curve was approached by multiple small sharp bents in the bending machine. Therefore the tape spring did not have a constant curvature, but it had locally high and low curvatures. The tool of the bending machine had a length of 0.5 m and therefore this process was done in two steps. This resulted in small dents in the middle of the tape spring, as shown in Fig. 15.

The produced tape springs had a tape spring radius of 19 mm, which is 2 mm smaller than specified. When the radius is too small, the stress within the tape spring will be too high, which results in plastic deformation. Because this plastic deformation was unavoidable, the tape spring were plastic deformed on purpose in a controlled way. This is done by first flatten the tape springs in transverse direction in a rolling machine. The next step was roll bending in longitudinal direction. The third step was folding the tape springs 180° by hand and applying the displacement over the whole range of motion.

This way of producing tape springs result in non-constant tape springs with a lot of imperfections. The force displacement behavior of the tape spring is however very sensitive for these imperfections. The peaks for example shown in Fig. 12 at 0.48 m and 0.58 m occurred at the moment the dents in the middle of the tape spring entered the bent region.

Therefore, future research should be done on how a tape spring should be produced.

CONCLUSION

Theoretically tape loops can be used to act as an all-purpose force generator. All fifteen unique force displacement behaviors could be obtained using the presented synthesis method.

The synthesis method only gives a rough estimation of the tape spring behavior. By using the knowledge of [11], the tape springs can be optimized for the desired behavior, which is done for a non-zero constant force tape loop.

The fabrication of tape springs however, remains challenging. Furthermore, tape springs are very sensitive for fabrication errors, which makes it even more challenging to produce tape springs which are able to act as force generators.

REFERENCES

[1] Calladine, C. R., 1988. "The theory of thin shell structures 1888-1988". *Institution of Mechanical Engineers,* ***202***(A3), pp. 141–149.

[2] Seffen, K. A., and Pellegrino, S., 1999. "Deployment dynamics of tape springs". *The Royal Society,* ***455***, pp. 1003–1048.

[3] Soykasap, Ö., 2007. "Analysis of tape spring hinges". *International Journal of Mechanical Sciences,* ***49***, pp. 853–860.

[4] Seffen, K. A., Pellegrino, S., and Parks, G. T., 2000. "Deployment of a Panel by Tape-Spring Hinges". In IUTAM-IASS Symposium on Deployable Structures: Theory and Applications, Kluwer Academic Publishers, pp. 355–364.

[5] Vehar, C., Kota, S., and Dennis, R., 2004. "Closed-Loop Tape Springs as Fully Compliant Mechanisms : Preliminary Investigations". In 28th Biennial Mechanisms and Robotics Conference, ASME, pp. 1–10.

[6] Houwers, H., 2016. "Closed-Loop Two-Fold Tape Spring Transmissions". Master thesis, Delft University of Technology.

[7] NASA, 1967. Rolamite: New Mechanical Design Concept. Tech. Rep. 67-10611, NASA, Springfield, Virginia.

[8] Cadman, R. V., 1970. Rolamite - Geometry and Force Analysis. Tech. rep., Sandia Laboratories, Albuquerque, N. Mex.

[9] English, C., and Russell, D., 1999. "Implementation of variable joint stiffness through antagonistic actuation using rolamite springs". *Mechanism and Machine Theory,* ***34***, pp. 27–40.

[10] Radaelli, G., 2017. "Synthesis of Mechanisms with Prescribed Elastic Load-Displacement Characteristics". Phd thesis, Delft University of Technology.

[11] de Jong, M. G., van de Sande, W. W., and Herder, J. L., 2018. "Influence of the Subtended Angle on the Behavior of Folded Tape Springs". In International Design Engineering Technical Conferences & Computers and Information in Engineering Conference, ASME, pp. 1–7.

5

Discussion

The first goal at the start was to find an analytical description of the total energy state of the tape spring with varying subtended angle. This analytical description was found for the bent region. For the energy in the transition region however, this was more complex. Several attempts were performed to describe the energy in the transition zones. The difficulty is that both the length of the transition regions and the distribution of the energy within the transition regions do not scale linearly with the subtended angle. In the end, a synthesis method without the transition regions could approach the required force displacement behavior. In order to synthesize the geometry for a given force displacement behavior exactly, the transition regions should be taken into account.

For the finite element simulation of the folded tape springs, a software package based on IGA was used. This software package turned out to be very sensitive for the given simulation parameters. The main parameters that influenced the solvability of the simulation were the number of time steps and the refine count of the geometry. When a wrong combination of parameters was used, the whole simulation did not solve. Therefore a lot of attempts needed to be made in order to find parameters that did solve. Eventually by using a cluster, a lot of simulations could be run simultaneously, which accelerated the process of finding the right parameters.

The tape springs for the experiment were not produced in an optimal way. The main problem was that the forming process of a thin spring steel plate with high yield strength is challenging, because of the high spring back. A possible way of improving the manufacturability is by performing the forming process before performing the hardening process of the steel plate. This can however results in unwanted and unknown prestresses in the material. Another difficulty was cutting the subtended angle profile in a curved steel plate. This problem could be solved by cutting the profile in a flat plate before applying the forming process. The downside of switching the processes is that the forming process will be more complicated. Another solution for the manufacturing problems could be using another material such as plastics or composites.

Although tape loops are promising, there are also several limitations. The hysteresis is very high, which can probably be caused by constant plastic deformation. When this is the case, a solution for the hysteresis could be using tape spring with a higher radius, because a higher radius would results in lower stresses and therefore no plastic deformation. Another drawback is that at higher scale, the weight of the tape loop itself becomes dominant. Therefore a tape loop at higher scale is not suitable for applications where the input motion is vertically. There is a trade-off between large energy storage and the range of motion. This is because the energy storage increases with higher subtended angles while the range of motion decreases. The length of the transitions regions and the energy within these regions does increase with higher subtended angles as well. While the transition regions are not incorporated into the synthesis method, this will results in synthesized geometry with less accurate force displacement behavior. Therefore the subtended angle should be preferably not too high.

Overall, when the production issues are solved, tape loops can be interesting for small scale applications where a simple monolithic solution is required.

6

Conclusion

In this thesis a method was presented to synthesize force generators with a custom force displacement behavior using two fold tape loops.

The thesis started with introducing a way to quantify the level of customizability of force generators with custom force displacement behavior. This method consists of fifteen force displacement curves that all describe a unique force displacement behavior, based on their force, stiffness and the derivative of stiffness which can either be positive, zero or negative. Eight different force generators with a custom force displacement curve were found and analyzed using these fifteen curves.

In the next chapter, the influence of varying the subtended angle on the behavior of folded tape springs was investigated. The two main subjects of the chapter were the energy state of the tape spring and the tape spring radius under influence of the subtended angle. It was discovered that a significant part of the strain energy is stored in the transition regions. The distribution of the energy between the transition region and the bent region is not constant for different subtended angles, while the part of the energy within the transition region gets larger for higher subtended angles. The fold radius that should be used for calculating the energy within the bent regions is found to be $\frac{7}{8}\pi$ instead of π. Another conclusion of this chapter is that the fold radius is not equal to the tape spring radius, despite suggestions otherwise in other papers. The fold radius even gets larger for smaller subtended angles which can be explained by that it starts to behave like a leaf spring. However, when the subtended angle is above 100 degrees, the fold radius remains nearly constant with a value of 5% larger than the tape spring radius. A tape loop can therefore act as a linear guide when keeping the subtended angle above 100 degrees.

In the fourth chapter, this knowledge was used to construct a synthesis method for the synthesis of a force generator with custom force displacement behavior using two fold tape loops. The fifteen unique force displacement curves that were presented in the second chapter were used as input of the synthesis model to calculate fifteen geometries. These resulting fifteen geometries were simulated in a finite element model to validate their behavior. The FEM model showed that all the synthesized geometries had similar force displacement behavior as the input of the synthesis method. The geometry with constant force behavior however still showed a small stiffness. Therefore that geometry was optimized for zero stiffness behavior. Using the knowledge of the second chapter, the geometry could be optimized for obtaining a non-zero constant force characteristic. This showed that 1) the synthesis method can be used to calculate geometries that approach the desired force displacement behavior and 2) tape loops with varying subtended angles can be used as force generator which can achieve all fifteen force displacement curves. The tape spring geometry with non-zero constant force behavior was produced and tested in the experiment. The produced tape spring with a constant subtended angle already had irregularities in its force displacement curve, while this geometry should results in a zero force and zero stiffness mechanism. Therefore the tape spring with the constant force geometry resulted in a force displacement path with irregularities as well. The force displacement path of this tape spring has made a shift upwards, which means that the geometry exerts a force. It can be

concluded that producing a tape spring is challenging while the force displacement curve of a tape spring is very sensitive to fabrication errors.

In conclusion, all fifteen unique force displacement behaviors can be obtained using tape loops, so therefore tape loops can be synthesized as all-purpose force generators.

Bibliography

[1] J. Herder, *Energy-free Systems. Theory, conception and design of statically balanced spring mechanisms*, Phd thesis, Delft University of Technology (2001).

[2] A. Ohtsuki, S. Oshima, and D. Itoh, *Analysis on Characteristics of a C-Shaped Constant-Force Spring with a Guide,* JSME **44**, 494 (2001).

[3] J. Van Eijk, *On the design of plate-spring mechanisms*, Phd thesis, Technische Hogeschool Delft (1985).

[4] R. L. Norton, *Cam Design and Manufacturing Handbook*, 2nd ed. (Industrial Press, Inc., New York, 2009) p. 640.

[5] H. Houwers, *Closed-Loop Two-Fold Tape Spring Transmissions*, Master thesis, Delft University of Technology (2016).